Substituting (7.16) into (7.17) gives

$$F(v) = \sum_k \int_a^b dv' \psi_k(v)\, \psi_k^*(v') F(v'). \tag{7.18}$$

This confirms (7.15) with

$$F_k = \int_a^b dv' \psi_k^*(v') F(v'). \tag{7.19}$$

Finally, consider $F(v) = \psi_j(v)$ in (7.15). This forces $F_k = \delta_{kj}$ and substitution into (7.19) gives the *orthonormality* relation

$$\int_a^b dv\, \psi_k^*(v) \psi_j(v) = \delta_{kj}. \tag{7.20}$$

7.5 Cartesian Symmetry

For potential problems with natural rectangular boundaries, the trial solution $\varphi(x, y, z) = X(x)Y(y)Z(z)$ converts Laplace's equation,

$$\nabla^2 \varphi = \frac{\partial^2 \varphi}{\partial x^2} + \frac{\partial^2 \varphi}{\partial y^2} + \frac{\partial^2 \varphi}{\partial z^2} = 0, \tag{7.21}$$

into

$$\frac{X''(x)}{X(x)} + \frac{Y''(y)}{Y(y)} + \frac{Z''(z)}{Z(z)} = 0. \tag{7.22}$$

Each of the three ratios in (7.22) is a function of only one variable. Therefore, their sum can be zero only if each is separately equal to a distinct constant. This gives

$$\frac{d^2X}{dx^2} = \alpha^2 X, \qquad \frac{d^2Y}{dx^2} = \beta^2 Y, \qquad \text{and} \qquad \frac{d^2Z}{dx^2} = \gamma^2 Z, \tag{7.23}$$

where the separation constants α^2, β^2, and γ^2 are real[5] and satisfy

$$\alpha^2 + \beta^2 + \gamma^2 = 0. \tag{7.24}$$

The methodology outlined in Section 7.4 directs us to identify all the elementary solutions of the differential equations in (7.23). The separation constants can be zero or non-zero, so

$$X_\alpha(x) = \begin{cases} A_0 + B_0 x & \alpha = 0, \\ A_\alpha e^{\alpha x} + B_\alpha e^{-\alpha x} & \alpha \neq 0, \end{cases} \tag{7.25}$$

$$Y_\beta(y) = \begin{cases} C_0 + D_0 y & \beta = 0, \\ C_\beta e^{\beta y} + D_\beta e^{-\beta y} & \beta \neq 0, \end{cases} \tag{7.26}$$

$$Z_\gamma(z) = \begin{cases} E_0 + F_0 z & \gamma = 0, \\ E_\gamma e^{\gamma z} + F_\gamma e^{-\gamma z} & \gamma \neq 0. \end{cases} \tag{7.27}$$

[5] The possibility that α, β, and γ are neither purely real nor purely imaginary is precluded by the boundary conditions for all the problems we will encounter in this book.

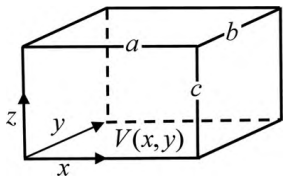

Figure 7.4: An empty box with five walls maintained at zero potential and the $z = 0$ bottom wall maintained at potential $V(x, y)$.

The linearity of Laplace's equation permits us to superpose the products of these elementary solutions. Therefore, using a delta function to enforce (7.24), the general solution reads

$$\varphi(x, y, z) = \sum_{\alpha} \sum_{\beta} \sum_{\gamma} X_\alpha(x) Y_\beta(y) Z_\gamma(z) \delta(\alpha^2 + \beta^2 + \gamma^2). \tag{7.28}$$

The form of (7.25) shows that α can be restricted to positive real values if $\alpha^2 > 0$ and to positive imaginary values if $\alpha^2 < 0$. Similar remarks apply to β and γ.

As an example, let us use (7.28) to find the electrostatic potential inside the rectangular box shown in Figure 7.4. We assume that all the walls are fixed at zero potential except for the $z = 0$ wall, where the potential takes specified values $V(x, y)$.[6] The homogeneous Dirichlet boundary conditions on the vertical side walls are not difficult to satisfy if we write $\alpha = i\alpha'$ and $\beta = i\beta'$ in (7.25) and (7.26). We then choose α', β', and the expansion coefficients to make $X_\alpha(x)$ and $Y_\beta(y)$ sine functions that vanish at $x = a$ and $y = b$, respectively. Bearing in mind the delta function constraint, (7.28) takes the form

$$\varphi(x, y, z) = \sum_{m=1}^{\infty} \sum_{n=1}^{\infty} \sin\left(\frac{m\pi x}{a}\right) \sin\left(\frac{n\pi y}{b}\right) \left[E_{mn} \exp(\gamma_{mn} z) + F_{mn} \exp(-\gamma_{mn} z)\right], \tag{7.29}$$

where

$$\gamma_{mn}^2 = \left(\frac{m\pi}{a}\right)^2 + \left(\frac{n\pi}{b}\right)^2. \tag{7.30}$$

Our next task is to choose E_{mn} and F_{mn} so the potential vanishes at $z = c$. If V_{mn} are coefficients still to be determined, a convenient way to write the result is

$$\varphi(x, y, z) = \sum_{m=1}^{\infty} \sum_{n=1}^{\infty} V_{mn} \sin\left(\frac{m\pi x}{a}\right) \sin\left(\frac{n\pi y}{b}\right) \frac{\sinh[\gamma_{mn}(c - z)]}{\sinh(\gamma_{mn} c)}. \tag{7.31}$$

It remains only to impose the final boundary condition that $\varphi(x, y, 0) = V(x, y)$. This gives

$$V(x, y) = \sum_{m=1}^{\infty} \sum_{n=1}^{\infty} V_{mn} \sin\left(\frac{m\pi x}{a}\right) \sin\left(\frac{n\pi y}{b}\right), \tag{7.32}$$

which is a double Fourier sine series representation of $V(x, y)$. To find the coefficients V_{mn}, multiply both sides of (7.32) by $\sin(m'\pi x/a) \sin(n'\pi y/b)$ and integrate over the intervals $0 \le x \le a$ and $0 \le y \le b$. This completes the problem because the orthogonality integral

$$\int_0^{\pi} ds \sin(ms) \sin(ns) = \frac{\pi}{2} \delta_{mn} \tag{7.33}$$

[6] We assume that a thin strip of insulating material isolates the bottom wall from the others.

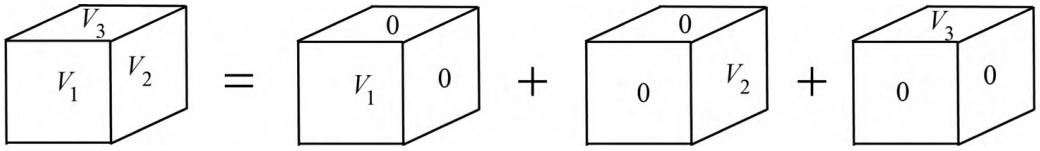

Figure 7.5: The potential in a box with three $\varphi = 0$ walls and three $\varphi \neq 0$ walls represented as the sum of three box potentials, each with five $\varphi = 0$ walls and one $\varphi \neq 0$ wall.

shows that

$$V_{mn} = \frac{4}{ab} \int_0^a \int_0^b dxdy\, V(x, y) \sin\left(\frac{m\pi x}{a}\right) \sin\left(\frac{n\pi y}{b}\right). \tag{7.34}$$

It was not an accident that a Fourier series appeared in (7.32) when the need arose to represent the arbitrary boundary data $V(x, y)$. The key was the homogeneous Dirichlet (zero potential) boundary condition imposed on each of the vertical walls in Figure 7.4. This transformed the differential equations for $X(x)$ and $Y(y)$ into eigenvalue problems with complete sets of orthogonal sine functions as their eigenfunctions.

Our example raises the question of how to "arrange" a complete set of eigenfunctions if we had specified non-zero potentials on any (or all) of the vertical side walls. The solution (indicated schematically in Figure 7.5) is to superpose the separated-variable solutions to several independent potential problems, each like the one we have just solved but with a different wall held at a non-zero potential. This general approach works for other coordinate systems also. Application 7.1 illustrates another method.

Application 7.1 A Conducting Duct

Figure 7.6 is a cross sectional view of an infinitely long, hollow, conducting duct. The walls are maintained at the constant potentials indicated and our task is to find the electrostatic potential everywhere inside the duct. A straightforward approach to this problem mimics Figure 7.5 and superposes the solutions of three different potential problems, each with only one wall held at a non-zero potential. The reader can confirm that only two problems actually need be superposed: one with $V' = 0$ and another with $V = 0$. In this Application, we follow a third path and use the $\beta = 0$ solution in (7.26) to remove the inhomogeneous boundary condition $\varphi(x, L) = V'$. More generally, we use a systematic "inspection" method which retains every elementary solution in (7.25), (7.26), and (7.27) until a boundary condition or other physical consideration forces us to remove it. Uniqueness guarantees that the solutions obtained by these three approaches will agree numerically at every point, despite their different analytic appearances.

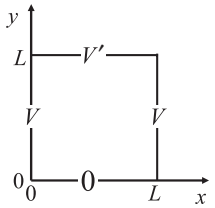

Figure 7.6: Cross sectional view of a conducting duct with Dirichlet boundary conditions.

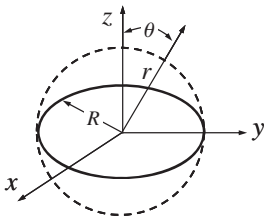

Figure 7.8: An origin-centered ring in the $z = 0$ plane with uniform charge per unit length $\lambda = Q/2\pi R$. The dashed sphere separates space into a region with $r < R$ and a region with $r > R$.

The zero-curvature condition guarantees that the solutions of Laplace's equation are not bounded in at least one Cartesian direction. Nevertheless, as both the duct and cage examples demonstrate, true divergence never occurs because a steadily increasing potential along some direction always signals the eventual appearance of a region of source charge where Laplace's equation is no longer valid. The only possible solution to $\nabla^2\varphi = 0$ in completely empty space is $\varphi = const.$, which corresponds to no electric field at all.

7.6 Azimuthal Symmetry

In Example 4.5, we found the potential of a uniformly charged ring (Figure 7.8) by evaluating all of its electrostatic multipole moments. Another way to solve this problem exploits separation of variables in spherical coordinates. The azimuthal symmetry of the ring implies that $\varphi(r, \theta, \phi) = \varphi(r, \theta)$. Therefore, for this problem (and any problem with azimuthal symmetry), the Laplace equation reduces to

$$\nabla^2\varphi = \frac{1}{r^2}\frac{\partial}{\partial r}\left(r^2\frac{\partial\varphi}{\partial r}\right) + \frac{1}{r^2\sin\theta}\frac{\partial}{\partial\theta}\left(\sin\theta\frac{\partial\varphi}{\partial\theta}\right) = 0. \tag{7.52}$$

With a change of variable to $x = \cos\theta$, the trial solution $\varphi(r, x) = R(r)M(x)$ separates (7.52) into the two ordinary differential equations

$$\frac{d}{dr}\left(r^2\frac{dR}{dr}\right) - \kappa R = 0 \tag{7.53}$$

and

$$\frac{d}{dx}\left[(1-x^2)\frac{dM}{dx}\right] + \kappa M = 0. \tag{7.54}$$

If we write the real separation constant as $\kappa = \nu(\nu+1)$, it is straightforward to verify that (7.53) is solved by

$$R_\nu(r) = A_\nu r^\nu + B_\nu r^{-(\nu+1)}. \tag{7.55}$$

The same substitution in (7.54) produces Legendre's differential equation:

$$(x^2-1)\frac{d^2M}{dx^2} + 2x\frac{dM}{dx} - \nu(\nu+1)M = 0. \tag{7.56}$$

The linearly independent solutions of (7.56) are called *Legendre functions* of the first and second kind. We denote them by $P_\nu(x)$ and $Q_\nu(x)$, respectively. This yields the general solution to Laplace's equation for a problem with azimuthal symmetry as

$$\varphi(r,\theta) = \sum_\nu \left[A_\nu r^\nu + B_\nu r^{-(\nu+1)}\right]\left[C_\nu P_\nu(\cos\theta) + D_\nu Q_\nu(\cos\theta)\right]. \tag{7.57}$$

For arbitrary values of ν, the Legendre functions have the property that $P_\nu(-1) = Q_\nu(\pm 1) = \infty$. These divergences are unphysical, so (7.57) in full generality applies only to problems where the domain of interest does not include the z-axis. An example is the space between two coaxial cones which open upward along the positive z-axis with their common vertex at the origin of coordinates. If we ask for the potential inside *one* such cone, (7.57) can include all the $P_\nu(x)$—but none of the $Q_\nu(x)$.

It remains only to provide a representation of the potential that can be used for problems where the entire z-axis is part of the physical domain. The answer turns out to be (7.57), provided we exclude the $Q_\nu(x)$ functions and restrict the values of ν to the non-negative integers, $\ell = 0, 1, 2, \ldots$. The latter choice reduces the $P_\nu(\cos\theta)$ functions to the Legendre polynomials $P_\ell(\cos\theta)$ (see Section 4.5.1), which are finite and well behaved over the entire angular range $0 \le \theta \le \pi$. The $Q_\ell(\cos\theta)$ functions remain singular at $\theta = \pi$.

7.6.1 A Uniformly Charged Ring

The charged ring in Figure 7.8 is a problem where the potential is required over the full angular range $0 \le \theta \le \pi$. In such a case, the preceding paragraph tells us that only the Legendre polynomials may appear in (7.57). Accordingly,

$$\varphi(r,\theta) = \sum_{\ell=0}^{\infty} \left[A_\ell r^\ell + B_\ell r^{-(\ell+1)}\right] P_\ell(\cos\theta). \tag{7.58}$$

On the other hand, neither r^ℓ nor $r^{-(\ell+1)}$ is finite throughout the entire radial domain $0 \le r < \infty$. This suggests a divide-and-conquer strategy: construct separate, regular solutions to Laplace's equation in the disjoint regions $r < R$ and $r > R$ and match them together at the surface of the ring ($r = R$). We will do this for a general (but specified) charge density $\sigma(\theta)$ applied to a spherical surface at $r = R$ and then specialize to the uniformly charged ring.

A representation which ensures that $\varphi(r,\theta)$ is both regular at the origin and goes to zero as $r \to \infty$ is

$$\varphi(r,\theta) = \begin{cases} \displaystyle\sum_{\ell=0}^{\infty} c_\ell \left(\frac{r}{R}\right)^\ell P_\ell(\cos\theta) & r \le R, \\ \displaystyle\sum_{\ell=0}^{\infty} c_\ell \left(\frac{R}{r}\right)^{\ell+1} P_\ell(\cos\theta) & r \ge R. \end{cases} \tag{7.59}$$

Notice that (7.59) builds in the continuity of the potential at $r = R$ as specified by (7.3). Using an obvious notation, the matching condition (7.4) is[9]

$$\epsilon_0 \left[\frac{\partial \varphi_<}{\partial r} - \frac{\partial \varphi_>}{\partial r}\right]_{r=R} = \sigma(\theta). \tag{7.60}$$

When applied to (7.59), this gives

$$\epsilon_0 \sum_{\ell=0}^{\infty} \frac{c_\ell}{R}(2\ell+1) P_\ell(\cos\theta) = \sigma(\theta). \tag{7.61}$$

[9] The representation (7.59) is valid for any value of R. We choose the radius of the ring in order to exploit the matching condition (7.60).

The final step is to multiply (7.61) by $P_m(\cos\theta)$ and integrate over the interval $0 \le \theta \le \pi$ using the orthogonality relation for the Legendre polynomials,

$$\int_{-1}^{1} dx\, P_\ell(x) P_m(x) = \frac{2}{2\ell+1}\delta_{\ell m}. \tag{7.62}$$

This yields the expansion coefficients in the form

$$c_m = \frac{R}{2\epsilon_0}\int_0^\pi d\theta\, \sin\theta\, \sigma(\theta) P_m(\cos\theta). \tag{7.63}$$

We infer from Example 4.5 that the surface charge density of the uniformly charged ring sketched in Figure 7.8 is $\sigma(\theta) = (\lambda/R)\,\delta(\cos\theta)$. Plugging this into (7.63) gives $c_m = Q P_m(0)/4\pi\epsilon_0 R$. Therefore, the electrostatic potential (7.59) of the ring is

$$\varphi(r,\theta) = \begin{cases} \dfrac{Q}{4\pi\epsilon_0}\displaystyle\sum_{\ell=0}^{\infty}\frac{r^\ell}{R^{\ell+1}} P_\ell(0) P_\ell(\cos\theta) & r \le R, \\[2ex] \dfrac{Q}{4\pi\epsilon_0}\displaystyle\sum_{\ell=0}^{\infty}\frac{R^\ell}{r^{\ell+1}} P_\ell(0) P_\ell(\cos\theta) & r \ge R. \end{cases} \tag{7.64}$$

This agrees with the multipole solution obtained in Example 4.5.

Application 7.2 Going Off the Axis

It is not absolutely necessary to use the matching condition (7.60) to find the expansion coefficients c_ℓ in (7.59). An alternative method exploits the uniqueness of the solutions to Laplace's equation. The idea is to compare the general formula (7.59) with an easily computable special case. For the latter, we let ϕ be the azimuthal variable, specialize to the charged ring, and use the Coulomb integral (7.1) to find the potential *on the z-axis*:

$$\varphi(z) = \frac{\lambda}{4\pi\epsilon_0}\int_0^{2\pi}\frac{R d\phi}{\sqrt{R^2+z^2}} = \frac{Q}{4\pi\epsilon_0}\frac{1}{\sqrt{R^2+z^2}}. \tag{7.65}$$

This expression can be rewritten using the generating function for the Legendre polynomials (see Section 4.5.1):

$$\frac{1}{\sqrt{1-2xt+t^2}} = \sum_{\ell=0}^{\infty} t^\ell P_\ell(x) \qquad |x| \le 1,\ 0 < t < 1. \tag{7.66}$$

When $|z| < R$, use of (7.66) with $x = 0$ in (7.65) gives

$$\varphi(z) = \frac{Q}{4\pi\epsilon_0}\frac{1}{\sqrt{R^2+z^2}} = \frac{Q}{4\pi\epsilon_0 R}\sum_{\ell=0}^{\infty}(z/R)^\ell P_\ell(0). \tag{7.67}$$

Comparing this with (7.59) specialized to the z-axis (where $r = z$ and $\theta = 0$) gives $c_\ell = Q P_\ell(0)/4\pi\epsilon_0 R$ as before because $P_\ell(1) = 1$. Given the c_ℓ, we can now use (7.59) to "go off the axis" and find the potential everywhere. This procedure shows that *any* azimuthally symmetric potential is uniquely determined by its values on the symmetry axis. ■

Example 7.2 In 1936, Lars Onsager constructed a theory of the dielectric constant for a polar liquid using a model of a point dipole $\mathbf{p}$ placed at the center of a spherical cavity of radius a scooped out of an infinite medium with dielectric constant κ. Find the electric field that acts on the dipole if the entire system is exposed to a uniform external electric field $\mathbf{E}_0 \parallel \mathbf{p}$.

Solution: Let the polar axis in spherical coordinates point along $\mathbf{E}_0$ and $\mathbf{p}$. The presence of the external field guarantees that $\varphi(r \to \infty) \to -E_0 r\cos\theta$. The presence of the point dipole at the center of the cavity guarantees that $\varphi(r \to 0) = p\cos\theta/(4\pi\epsilon_0 r^2)$. Everywhere else, the potential satisfies Laplace's equation. Therefore, because both sources behave as $P_1(\cos\theta) = \cos\theta$, only $\cos\theta$ terms can be present in the general solution (7.59). In other words,

$$\varphi(r) = \begin{cases} \left[Ar + \dfrac{p}{4\pi\epsilon_0 r^2}\right]\cos\theta & r \le a, \\ \left[-E_0 r + \dfrac{B}{r^2}\right]\cos\theta & r \ge a. \end{cases}$$

There is no free charge at the cavity boundary, so the matching conditions (7.3) and (7.4) are

$$\varphi_{\text{in}}(a,\theta) = \varphi_{\text{out}}(a,\theta) \qquad \left.\frac{\partial\varphi_{\text{in}}}{\partial r}\right|_{r=a} = \kappa \left.\frac{\partial\varphi_{\text{out}}}{\partial r}\right|_{r=a}.$$

Therefore, we find without complication that

$$A = -\frac{3\kappa}{2\kappa+1}E_0 - \frac{2p}{4\pi\epsilon_0 a^3}\frac{\kappa-1}{2\kappa+1} \qquad \text{and} \qquad B = -a^3 E_0\frac{\kappa-1}{2\kappa+1} + \frac{p}{4\pi\epsilon_0}\frac{3}{2\kappa+1}.$$

The electric field that acts on the dipole is $\mathbf{E} = -\nabla\varphi$ for $r \le a$ minus the contribution from $\mathbf{p}$ itself:

$$\mathbf{E}(0) = \frac{3\kappa}{2\kappa+1}\mathbf{E}_0 + \frac{2\mathbf{p}}{4\pi\epsilon_0 a^3}\frac{\kappa-1}{2\kappa+1}.$$

7.7 Spherical Symmetry

In this section, we solve Laplace's equation for problems with natural spherical boundaries that lack full azimuthal symmetry. These situations require the complete Laplacian operator in spherical coordinates:

$$\nabla^2\varphi = \frac{1}{r^2}\frac{\partial}{\partial r}\left(r^2\frac{\partial\varphi}{\partial r}\right) + \frac{1}{r^2\sin\theta}\frac{\partial}{\partial\theta}\left(\sin\theta\frac{\partial\varphi}{\partial\theta}\right) + \frac{1}{r^2\sin^2\theta}\frac{\partial^2\varphi}{\partial\phi^2} = 0. \tag{7.68}$$

The trial solution $\varphi(r,\theta,\phi) = R(r)Y(\theta,\phi)$ separates (7.68) into the ordinary differential equation

$$\frac{d}{dr}\left(r^2\frac{dR}{dr}\right) = \ell(\ell+1)R \tag{7.69}$$

and the partial differential equation

$$-\frac{1}{\sin\theta}\frac{\partial}{\partial\theta}\left(\sin\theta\frac{\partial Y}{\partial\theta}\right) - \frac{1}{\sin^2\theta}\frac{\partial^2 Y}{\partial\phi^2} = \ell(\ell+1)Y. \tag{7.70}$$

The choice of the separation constant as $\ell(\ell+1)$ allows us to borrow the solution of the radial equation (7.69) from Section 7.6:

$$R_\ell(r) = A_\ell r^\ell + B_\ell r^{-(\ell+1)}. \tag{7.71}$$

The notation indicates that we have already specialized to the case where ℓ is a non-negative integer. In practice, this case applies to the vast majority of non-contrived electrostatics problems with spherical boundaries. Moreover, when $\ell = 0, 1, 2, \ldots$, (7.70) is exactly the eigenvalue equation for the (dimensionless) quantum mechanical orbital angular momentum operator $\hat{L}^2$:

$$\hat{L}^2 Y_{\ell m}(\theta, \phi) = \ell(\ell + 1) Y_{\ell m}(\theta, \phi). \tag{7.72}$$

The complex-valued eigenfunctions $Y_{\ell m}(\theta, \phi)$ are the *spherical harmonics* introduced in Section 4.5.2. From the point of view of separation of variables, the constant m^2 separates (7.70) into two ordinary differential equations when we write $Y(\theta, \phi) = B(\theta)G(\phi)$. The choice of m as an integer in the range $-\ell \leq m \leq \ell$ guarantees that the spherical harmonics are finite and well behaved when $0 \leq \theta < \pi$ and $0 \leq \phi < 2\pi$. Appendix C gives a table of spherical harmonics and lists a few of their properties. Here, we exhibit only the orthogonality integral,[10]

$$\int d\Omega \; Y^*_{\ell' m'}(\Omega) Y_{\ell m}(\Omega) = \delta_{\ell \ell'} \delta_{m m'}, \tag{7.73}$$

and the phase relation

$$Y_{\ell, -m}(\theta, \phi) = (-)^m Y^*_{\ell m}(\theta, \phi). \tag{7.74}$$

Combining all the above, the general solution to Laplace's equation in spherical coordinates is

$$\varphi(r, \theta, \phi) = \sum_{\ell=0}^{\infty} \sum_{m=-\ell}^{\ell} \left[A_{\ell m} r^{\ell} + B_{\ell m} r^{-(\ell+1)} \right] Y_{\ell m}(\theta, \phi). \tag{7.75}$$

A typical problem requires a partition of the radial space as in (7.59) to ensure that the solution is regular at the origin and at infinity. Thus, (7.75) shows why the exterior multipole expansion (4.86) represents the potential for $r > R$ when charge occurs only *inside* an origin-centered sphere of radius R:

$$\varphi(r, \theta, \phi) = \frac{1}{4\pi\epsilon_0} \sum_{\ell=0}^{\infty} \sum_{m=-\ell}^{\ell} A_{\ell m} \frac{Y_{\ell m}(\theta, \phi)}{r^{\ell+1}} \qquad r > R. \tag{7.76}$$

The solution (7.75) also shows why the interior multipole expansion (4.89) represents the potential for $r < R$ when charge occurs only *outside* an origin-centered sphere of radius R:

$$\varphi(r, \theta, \phi) = \frac{1}{4\pi\epsilon_0} \sum_{\ell=0}^{\infty} \sum_{m=-\ell}^{\ell} B_{\ell m} r^{\ell} Y^*_{\ell m}(\theta, \phi) \qquad r < R. \tag{7.77}$$

These expansions are valid only in regions of space *free* from the source charge which defines the multipole moments $A_{\ell m}$ and $B_{\ell m}$.

Application 7.3 The Unisphere

The stainless steel "Unisphere" is the largest representation of the Earth ever constructed (Figure 7.9). Let this object be a model for a spherical conducting shell from which finite portions of the surface have been removed. The real Unisphere is grounded for safety. Here, we assume the shell is charged to a potential φ_0 and show that the *difference* in the surface charge density inside and outside the shell is a *constant* over the entire surface.

[10] $d\Omega \equiv \sin\theta d\theta d\phi$.

Figure 7.9: The "Unisphere" was the symbol of the 1964 World's Fair. The sphere radius is $R \approx 18$ m. Photograph from www.fotocommunity.de.

Place the origin of coordinates at the center of the shell. A representation that guarantees that $\varphi(\mathbf{r})$ is regular, continuous, and satisfies Laplace's equation everywhere off the shell is

$$\varphi(r,\theta,\phi) = \begin{cases} \displaystyle\sum_{\ell m} A_{\ell m} \left(\frac{r}{R}\right)^{\ell} Y_{\ell m}(\theta,\phi) & r \le R, \\ \displaystyle\sum_{\ell m} A_{\ell m} \left(\frac{R}{r}\right)^{\ell+1} Y_{\ell m}(\theta,\phi) & r \ge R. \end{cases} \tag{7.78}$$

The Dirichlet boundary condition is

$$\varphi_0 = \sum_{\ell m} A_{\ell m}\, Y_{\ell m}(\theta,\phi)|_{\text{on}}\,, \tag{7.79}$$

where the subscript "on" indicates that the equality holds only for angles (θ,ϕ) which coincide with the conducting surface of the shell. Therefore, the charge density difference $\Delta\sigma(\theta,\phi) = \sigma_{\text{out}}(\theta,\phi) - \sigma_{\text{in}}(\theta,\phi)$ between the outer and inner surfaces of the shell is

$$\Delta\sigma(\theta,\phi) = \epsilon_0 \left[\frac{\partial\varphi_>}{\partial r} + \frac{\partial\varphi_<}{\partial r}\right]_{\text{on}} = -\frac{\epsilon_0}{R}\sum_{\ell m} A_{\ell m}\, Y_{\ell m}(\theta,\phi)|_{\text{on}} = -\frac{\epsilon_0\,\varphi_0}{R}. \tag{7.80}$$

As advertised, this is indeed a constant, independent of (θ,ϕ). ■

Example 7.3 An origin-centered sphere has radius R. Find the volume charge density $\rho(r,\theta,\phi)$ (confined to $r < R$) and the surface charge density $\sigma(\theta,\phi)$ (confined to $r = R$) which together produce the electric field given below. Express the answer using trigonometric functions.

$$\mathbf{E} = -\frac{2V_0 x}{R^2}\hat{\mathbf{x}} + \frac{2V_0 y}{R^2}\hat{\mathbf{y}} - \frac{V_0}{R}\hat{\mathbf{z}} \qquad x^2+y^2+z^2 \le R^2.$$

Solution: Integrating each component of $\mathbf{E} = -\nabla\varphi$ gives

$$\begin{aligned} \hat{x}: &\qquad \varphi = \frac{V_0}{R^2}x^2 + f(y,z) \\ \hat{y}: &\qquad \varphi = -\frac{V_0}{R^2}y^2 + g(x,z) \\ \hat{z}: &\qquad \varphi = \frac{V_0}{R}z + h(x,y). \end{aligned}$$

Therefore,

$$\varphi_{\text{in}}(x, y, z) = \frac{V_0}{R^2}\left(x^2 - y^2\right) + \frac{V_0}{R}z + const. \qquad x^2 + y^2 + z^2 \le R^2.$$

Direct computation in Cartesian coordinates shows that φ_{in} satisfies Laplace's equation. Since $\rho = -\epsilon_0\nabla^2\varphi$, we conclude that there is no volume charge inside the sphere. On the other hand, in spherical coordinates, we know that solutions of Laplace's equation take the form (7.78). This means that the $x^2 - y^2$ term in φ_{in} is (at worst) a linear combination of $\ell = 2$ terms. The z term in φ_{in} is an $\ell = 1$ term. Therefore, because $x = r\sin\theta\cos\phi$, $y = r\sin\theta\sin\phi$, and $z = r\cos\theta$,

$$\varphi(r, \theta, \phi) = \begin{cases} V_0\dfrac{r}{R}\cos\theta + V_0\left(\dfrac{r}{R}\right)^2\sin^2\theta\cos 2\phi & r \le R, \\ V_0\left(\dfrac{R}{r}\right)^2\cos\theta + V_0\left(\dfrac{R}{r}\right)^3\sin^2\theta\cos 2\phi & r \ge R. \end{cases}$$

The charge density follows from the matching condition

$$\sigma(\theta, \phi) = \epsilon_0\left[\frac{\partial\varphi_{\text{in}}}{\partial r} - \frac{\partial\varphi_{\text{out}}}{\partial r}\right]_{r=R} = \epsilon_0\frac{V_0}{R}\left(3\cos\theta + 5\sin^2\theta\cos 2\phi\right).$$

7.8 Cylindrical Symmetry

Laplace's equation in cylindrical coordinates is

$$\nabla^2\varphi = \frac{1}{\rho}\frac{\partial}{\partial\rho}\left(\rho\frac{\partial\varphi}{\partial\rho}\right) + \frac{1}{\rho^2}\frac{\partial^2\varphi}{\partial\phi^2} + \frac{\partial^2\varphi}{\partial z^2} = 0. \tag{7.81}$$

For problems with cylindrical boundaries or, more generally, for problems with a unique preferred axis, the trial solution $\varphi(\rho, \phi, z) = R(\rho)G(\phi)Z(z)$ separates (7.81) into three ordinary differential equations with two real separation constants α^2 and k^2:

$$\rho\frac{d}{d\rho}\left(\rho\frac{dR}{d\rho}\right) + (k^2\rho^2 - \alpha^2)R = 0 \tag{7.82}$$

$$\frac{d^2G}{d\phi^2} + \alpha^2 G = 0 \tag{7.83}$$

$$\frac{d^2Z}{dz^2} - k^2 Z = 0. \tag{7.84}$$

Boundary and regularity (finiteness) conditions may or may not decide for us whether to choose α^2 and k^2 positive or negative. If both are chosen positive, the elementary solutions for $G(\phi)$ and $Z(z)$ are

$$G_\alpha(\phi) = \begin{cases} x_0 + y_0\phi & \alpha = 0, \\ x_\alpha\exp(i\alpha\phi) + y_\alpha\exp(-i\alpha\phi) & \alpha \ne 0, \end{cases} \tag{7.85}$$

and

$$Z_k(z) = \begin{cases} s_0 + t_0 z & k = 0, \\ s_k\exp(kz) + t_k\exp(-kz) & k \ne 0. \end{cases} \tag{7.86}$$

7.8.1 Bessel Functions

The radial equation (7.82) is Bessel's differential equation. If we let $k = i\kappa$, the elementary solutions of this equation are

$$R_\alpha^k(\rho) = \begin{cases} A_0 + B_0 \ln \rho & k = 0, \quad \alpha = 0, \\ A_\alpha \rho^\alpha + B_\alpha \rho^{-\alpha} & k = 0, \quad \alpha \neq 0, \\ A_\alpha^k J_\alpha(k\rho) + B_\alpha^k N_\alpha(k\rho) & k^2 > 0, \\ A_\alpha^k I_\alpha(\kappa\rho) + B_\alpha^k K_\alpha(\kappa\rho) & k^2 < 0. \end{cases} \tag{7.87}$$

$J_\alpha(x)$ and $N_\alpha(x)$ are called *Bessel functions* of the first and second kind, respectively. The *modified Bessel functions* $I_\alpha(x)$ and $K_\alpha(x)$ are Bessel functions with pure imaginary arguments:

$$I_\alpha(\kappa\rho) = i^{-\alpha} J_\alpha(ik\rho) \qquad K_\alpha(\kappa\rho) = \frac{\pi}{2} i^{\alpha+1}[J_\alpha(ik\rho) + iN_\alpha(ik\rho)]. \tag{7.88}$$

We define $J_\alpha(x)$, $N_\alpha(x)$, $I_\alpha(x)$, and $K_\alpha(x)$ for $x \geq 0$ only and refer the reader to Appendix C for more information. However, when α is real, it is important to know that $J_\alpha(x)$ is regular everywhere, $N_\alpha(x)$ diverges as $x \to 0$, and the asymptotic behavior ($x \gg 1$) of both is damped oscillatory:

$$\begin{aligned} J_\alpha(x) &\to \sqrt{\frac{2}{\pi x}}\ \cos(x - \alpha\pi/2 - \pi/4) \\ N_\alpha(x) &\to \sqrt{\frac{2}{\pi x}}\ \sin(x - \alpha\pi/2 - \pi/4). \end{aligned} \tag{7.89}$$

The modified Bessel function $I_\alpha(x)$ is finite at the origin and diverges exponentially as $x \to \infty$. $K_\alpha(x)$ diverges as $x \to 0$ but goes to zero exponentially as $x \to \infty$.

The general solution of Laplace's equation in cylindrical coordinates is a linear combination of the elementary solutions

$$\varphi(\rho, \phi, z) = \sum_\alpha \sum_k R_\alpha^k(\rho) G_\alpha(\phi) Z_k(z). \tag{7.90}$$

The results of the previous paragraph show that the choice $k^2 > 0$ produces a solution (7.90) which pairs oscillatory Bessel function behavior for $R(\rho)$ with real exponential functions for $Z(z)$. Conversely, the choice $k^2 < 0$ pairs a Fourier representation for $Z(z)$ with modified Bessel functions and thus real exponential behavior for $R(\rho)$. The fact that $\varphi(\rho, \phi, z)$ always exhibits simultaneous oscillatory and exponential behavior in its non-angular variables is the cylindrical manifestation of the "zero-curvature" property of the solutions to Laplace's equation discussed in Section 7.5.2. Finally, the matching conditions produce two natural constraints on the angular variation in (7.90). The first, $G(0) = G(2\pi)$, is a consequence of the continuity of the potential (7.3). The second, $G'(0) = G'(2\pi)$, is a consequence of (7.4) if the full angular range $0 \leq \phi \leq 2\pi$ is free of charge. Using (7.85), both conditions together force $\alpha = n$ where $n = 0, 1, 2, \ldots$ is a non-negative integer.

7.8.2 Fourier-Bessel Series

An interesting class of potential problems asks us to solve $\nabla^2\varphi = 0$ inside a cylinder of radius R when the potential is specified on two cross sections, say, $\varphi(\rho \leq R, \phi, z = z_1) = f_1(\rho, \phi)$ and $\varphi(\rho \leq R, \phi, z = z_2) = f_2(\rho, \phi)$. In the spirit of the problem defined by Figure 7.4, this calls for complete sets of eigenfunctions in the variables ρ and ϕ. Periodic boundary conditions are appropriate for the angular variable and a glance at (7.85) shows that the functions $G_m(\phi) = \exp(im\phi)$ suffice if $m = 0, \pm 1, \pm 2, \ldots$ This forces $\alpha = m$ in (7.87) and we are further restricted to functions $R_m^k(\rho)$ which are finite at the origin. Accordingly, the radial eigenfunctions are the set of functions which satisfy the homogeneous boundary condition $J_m(kR) = 0$. This condition fixes the allowed values

of the separation constant at $k_{mn} = x_{mn}/R$ where x_{mn} is the nth zero of the Bessel function $J_m(x)$. Invoking completeness, we conclude it must be possible to construct a *Fourier-Bessel series* where, say,

$$f_1(\rho, \phi) = \sum_{m=-\infty}^{\infty} \sum_{n=1}^{\infty} c_{mn} J_m(x_{mn}\rho/R) \exp(im\phi). \tag{7.91}$$

To compute the c_{mn}, multiply both sides of (7.91) by $\rho J_m(k_m n'\rho) \exp(-im'\phi)$ and integrate over the intervals $0 \le \rho \le R$ and $0 \le \phi < R$. This is sufficient because the exponential and Bessel functions satisfy the orthogonality relations

$$\frac{1}{2\pi} \int_0^{2\pi} d\phi \, e^{i(m-m')\phi} = \delta_{mm'} \tag{7.92}$$

and

$$\int_0^R d\rho \, \rho J_m(k_{mn}\rho) J_m(k_{mn'}\rho) = \delta_{nn'} \frac{1}{2} R^2 [J_{m+1}(k_{mn}R)]^2. \tag{7.93}$$

Application 7.4 An Electrostatic Lens

In 1931, Davisson and Calbick discovered that a circular hole in a charged metal plate focuses electrons exactly like an optical lens focuses light.[11] In fact, all electrostatic potentials with cylindrical symmetry have this property. Figure 7.10 shows another common electron lens: two adjacent and coaxial metal tubes of radius R separated by a small gap d. A potential difference $V_R - V_L$ is maintained between the tubes. In this Application, we calculate the potential inside the tubes (in the $d \to 0$ limit) and briefly discuss their focusing properties.

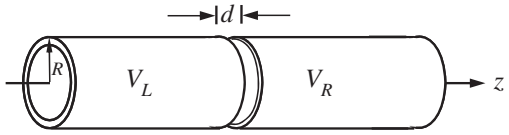

Figure 7.10: A two-tube electron lens.

If we separate variables in Laplace's equation in cylindrical coordinates, the rotational symmetry of the tubes fixes the separation constant in (7.83) at $\alpha = 0$. The choices $x_0 = 1$ and $y_0 = 0$ in (7.85) reduce $\varphi(\rho, \phi, z)$ to $\varphi(\rho, z)$. Here, we write $k = i\kappa$ and show (by construction) that the problem can be solved using radial functions with $k^2 < 0$ only. We invite the reader to show that a solution which looks different (but which is numerically equal by uniqueness) can be constructed using only radial functions with $k^2 > 0$. The potential must be finite at $\rho = 0$. Therefore, the discussion in Section 7.8.1 tells us that the most general form of the potential at this point is

$$\varphi(\rho, z) = \frac{1}{2\pi} \int_{-\infty}^{-\infty} d\kappa \, A(\kappa) I_0(|\kappa|\rho) e^{i\kappa z} + const. \tag{7.94}$$

The extracted factor of 2π emphasizes that (7.94) is a Fourier integral. Therefore, an application of Fourier's inversion theorem (i.e., the orthogonality of the complex exponential functions) gives

$$A(\kappa) = \frac{1}{I_0(|\kappa|\rho)} \int_{-\infty}^{\infty} dz \, \varphi(\rho, z) e^{-i\kappa z}. \tag{7.95}$$

[11] C.J. Davisson and C.J. Calbick, "Electron lenses", *Physical Review* **38**, 585 (1931).

To evaluate (7.95), we let $d \to 0$ in Figure 7.10 so $\varphi(R, z) = V_L$ when $z < 0$ and $\varphi(R, z) = V_R$ when $z > 0$. This gives[12]

$$A(\kappa) = \frac{1}{I_0(|\kappa|R)} \left[V_L \int_{-\infty}^{0} dz\, e^{-i\kappa z} + V_R \int_{0}^{\infty} dz\, e^{-i\kappa z} \right] = \frac{1}{i\kappa} \frac{V_R - V_L}{I_0(|\kappa|R)}. \tag{7.96}$$

Consequently,

$$\varphi(\rho, z) = \frac{V_R - V_L}{2\pi i} \int_{-\infty}^{\infty} \frac{d\kappa}{\kappa} \frac{I_0(|\kappa|\rho)}{I_0(|\kappa|R)} e^{i\kappa z} + const. \tag{7.97}$$

The real part of the integrand in (7.97) is an odd function of κ. Therefore, the potential inside the tube is

$$\varphi(\rho, z) = \frac{V_R + V_L}{2} + \frac{V_R - V_L}{\pi} \int_{0}^{\infty} \frac{d\kappa}{\kappa} \frac{I_0(\kappa\rho)}{I_0(\kappa R)} \sin \kappa z. \tag{7.98}$$

The additive constant in (7.97) was chosen to make $\varphi(\rho, 0) = \frac{1}{2}(V_R + V_L)$ in (7.98).

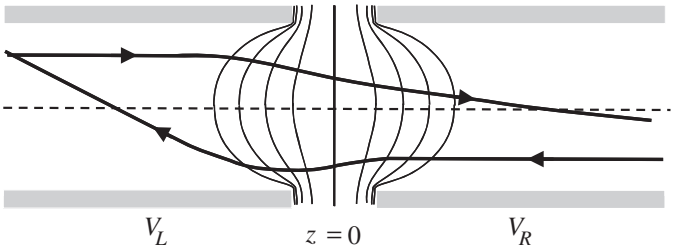

Figure 7.11: A two-tube electron lens with the symmetry axis (dashed) and a few equipotentials (light solid lines) indicated. The heavy solid lines are two particle trajectories drawn for $V_R > V_L$. Figure adapted from Heddle (1991).

Figure 7.11 is a cut-open view of the two tubes with a few equipotentials of (7.98) drawn as light solid lines. The dark solid lines are the trajectories of two charged particles. Although they move in opposite directions, both initially follow straight-line paths parallel to the z-axis in the $\mathbf{E} = 0$ region inside one tube. Both particles bend in the vicinity of the gap and then cross the z-axis during subsequent straight-line motion in the $\mathbf{E} = 0$ region of the other tube. In the language of optics, the $\mathbf{E} \neq 0$ regions of space on opposite sides of $z = 0$ deflect particles moving from left to right in Figure 7.11 first like a converging lens and then like a diverging lens. Particles moving from right to left are deflected first like a diverging lens and then like a converging lens. The diverging effect is weaker than the converging effect.[13] Therefore, particles are always focusing toward the symmetry axis on the far side of the gap. ■

7.9 Polar Coordinates

There are many physical situations where the electrostatic potential is effectively a function of two (rather than three) spatial variables. The conducting duct (Application 7.1) and the Faraday cage (Section 7.5.1) are examples we solved in Cartesian coordinates. When the symmetry of the problem

[12] We use the regularization $\int_0^{\pm\infty} dz\, e^{-i\kappa z} = \lim_{\alpha \to 0} \int_0^{\pm\infty} dz\, e^{-i\kappa z} e^{\mp \alpha z}$.

[13] We leave it as an exercise for the reader to show that this is a generic feature of charged particle motion near the symmetry axis of a cylindrical potential.

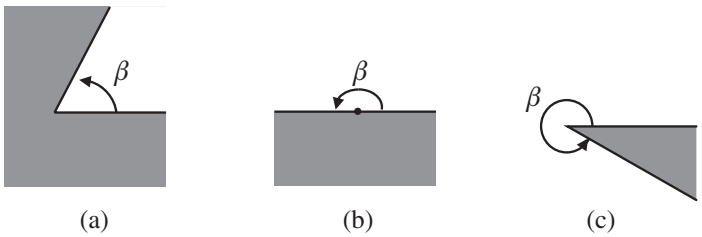

Figure 7.12: Side view of a two-dimensional wedge ($0 \le \phi \le \beta$) cut out of perfectly conducting (shaded) matter. The conductor is held at zero potential and otherwise fills all of space.

warrants it, it may be more natural to study separated-variable solutions of the two-dimensional Laplace's equation written in polar coordinates,

$$\nabla^2\varphi = \frac{1}{\rho}\frac{\partial}{\partial\rho}\left(\rho\frac{\partial\varphi}{\partial\rho}\right) + \frac{1}{\rho^2}\frac{\partial^2\varphi}{\partial\phi^2} = 0. \tag{7.99}$$

Alternatively, a general, separated-variable solution to (7.99) follows from the cylindrical-coordinates solution (7.90) with $Z(z) = 1$ and $k = 0$. If we switch from exponential functions to sinusoidal functions of the polar angle ϕ, the result can be written

$$\varphi(\rho,\phi) = (A_0 + B_0\ln\rho)(x_0 + y_0\phi) + \sum_{\alpha\neq 0}[A_\alpha\rho^\alpha + B_\alpha\rho^{-\alpha}][x_\alpha\sin\alpha\phi + y_\alpha\cos\alpha\phi]. \tag{7.100}$$

If, say, the potential far from the origin were due to a uniform electric field $\mathbf{E} = E_0\hat{\mathbf{x}}$, it would be necessary to put $B_0 = A_\alpha = 0$ except for the single term $E_0\rho\cos\phi$.

7.9.1 The Electric Field near a Sharp Corner or Edge

The electric field $\mathbf{E}(\rho,\phi)$ inside a two-dimensional wedge ($0 \le \phi \le \beta$) bounded by a grounded perfect conductor (Figure 7.12) provides insight into the nature of electric fields near sharp conducting corners. The potential cannot be singular as $\rho \to 0$ so (7.100) simplifies to

$$\varphi(\rho,\phi) = A + B\phi + \sum_{\alpha>0} C_\alpha\rho^\alpha\sin(\alpha\phi + \delta_\alpha). \tag{7.101}$$

We get $A = B = 0$ because $\varphi(0,\phi) = 0$. Moreover, $\varphi(\rho,0) = \varphi(\rho,\beta) = 0$ implies that $\delta_\alpha = 0$ and $\alpha = m\pi/\beta$ where m is a positive integer. The coefficients C_m are determined by boundary or matching conditions far from $\rho = 0$ which we do not specify. On the other hand, the $m = 1$ term dominates the sum as $\rho \to 0$. Therefore, up to a multiplicative constant, the potential very near the apex is

$$\varphi(\rho,\phi) \approx \rho^{\pi/\beta}\sin(\pi\phi/\beta). \tag{7.102}$$

The associated electric field is

$$\mathbf{E} = -\nabla\varphi = -\frac{\pi}{\beta}\rho^{\pi/\beta-1}\left\{\hat{\boldsymbol{\rho}}\sin(\pi\phi/\beta) + \hat{\boldsymbol{\phi}}\cos(\pi\phi/\beta)\right\}. \tag{7.103}$$

Equation (7.103) correctly gives $\mathbf{E}$ as a vertically directed constant vector when $\beta = \pi$ [Figure 7.12(b)]. Otherwise, $|\mathbf{E}| \to 0$ as $\rho \to 0$ when $\beta < \pi$ [Figure 7.12(a)] but $|\mathbf{E}| \to \infty$ as $\rho \to 0$ when $\beta > \pi$ [Figure 7.12(c)]. This singular behavior is not new: we saw in (5.33) that the surface charge density of a conducting disk has a square-root singularity at its edge. This is consistent with the

electric field here in the limit $\beta \to 2\pi$. A related singularity is often invoked to explain the behavior of a lightning rod.[14]

Analogy with Gas Diffusion

Imagine a collection of gas particles that *diffuse* from infinity toward the wedge in Figure 7.12. Each particle sticks to the wedge at the point of impact. The space and time dependence of the gas density $n(\mathbf{r}, t)$ is governed by the diffusion constant D and the diffusion equation, $D\nabla^2 n = \partial n/\partial t$. If we continuously supply gas from infinity, the density quickly reaches a time-independent steady state governed by $\nabla^2 n(\mathbf{r}) = 0$. The boundary condition for this equation is $n(\mathbf{r}_S) = 0$ at the wedge surface because "sticking" irreversibly removes particles from the gas. This establishes a one-to-one correspondence between the steady-state gas diffusion problem and the electrostatic problem solved just above. The analog of the electric field for the gas problem is the particle number current density $\mathbf{j}(\mathbf{r}) = -D\nabla n$. Now recall that diffusing particles execute a random walk in space. When $\beta > \pi$, such particles are very likely to encounter the convex apex before any other portion of the wedge, i.e., there is a large flux of particles to the apex. Conversely, when $\beta < \pi$, diffusing particles are very *unlikely* to reach the concave corner before striking another portion of the wedge. The net particle flux to the corner is very small. These are precisely the behaviors exhibited by $\mathbf{E}(\mathbf{r})$ near the apex.

Example 7.4 Find $\varphi(\rho, \phi)$ in the region bounded by the two arcs $\rho = \rho_1$ and $\rho = \rho_2$ and the two rays $\phi = \phi_1$ and $\phi = \phi_2$. All the boundaries are grounded except that $\varphi(\rho, \phi_2) = f(\rho)$. How does the nature of the separation constant change in the limit $\rho_1 \to 0$?

Solution: The homogeneous boundary conditions $\varphi(\rho_1, \phi) = \varphi(\rho_2, \phi) = 0$ eliminate the $\alpha = 0$ terms in the general solution (7.100). On the other hand, it seems impossible to satisfy these boundary conditions using the functions ρ^α and $\rho^{-\alpha}$ until we realize that $\rho^{\pm\alpha} = \exp(\pm\alpha \ln \rho)$. The choice $\alpha = i\gamma$ then turns the ρ dependence of (7.100) into a Fourier series in the variable $\ln \rho$. The general solution at this point is

$$\varphi(\rho, \phi) = \sum_{\gamma \neq 0} (A_\gamma e^{i\gamma \ln \rho} + B_\gamma e^{-i\gamma \ln \rho})(x_\gamma \sinh \gamma\phi + y_\gamma \cosh \gamma\phi).$$

We satisfy $\varphi(\rho_2, \phi) = 0$ by choosing the ratio A_γ/B_γ so the radial functions are $\sin\{\gamma \ln(\rho/\rho_2)\}$. We satisfy $\varphi(\rho_1, \phi) = 0$ by choosing $\gamma = m\pi/\ln(\rho_1/\rho_2)$ where m is an integer. The condition $\varphi(r, \phi_1) = 0$ leads to

$$\varphi(\rho, \phi) = \sum_{m=-\infty}^{\infty} A_m \sin\left\{\frac{m\pi \ln(\rho/\rho_2)}{\ln(\rho_1/\rho_2)}\right\} \sinh\left\{\frac{m\pi(\phi - \phi_1)}{\ln(\rho_1/\rho_2)}\right\}.$$

Finally, let $\theta = \pi \ln(\rho/\rho_2)/\ln(\rho_1/\rho_2)$, multiply both sides of the foregoing by $\sin(n\theta)$, and integrate over the interval $0 \leq \theta \leq \pi$. This completes the solution because the orthogonality of the sine functions uniquely determines the A_m.

[14] The field is very large but not truly singular near a rounded edge or near the tip of a lighting rod. Our analysis is approximately valid as long as the edge or tip is spatially isolated from other parts of the conductor and the radius of curvature of the edge or tip is small compared to any other length scale in the problem.